NIH Public Access
Author Manuscript
Dev Dyn. Author manuscript; available in PMC 2013 December 01.

Published in final edited form as:
Dev Dyn. 2012 December ; 241(12): 1922–1932. doi:10.1002/dvdy.23877.

Structural disorganization of pronephric glomerulus in zebrafish *mpp5a/nagie oko* mutant

Koichiro Ichimura[1,2], **Yayoi Fukuyo**[1], **Tomomi Nakamura**[1,3], **Rebecca Powell**[1], **Tatsuo Sakai**[2], and **Tomoko Obara**[1,*]

[1]Department of Cell Biology, University of Oklahoma Health Science Center, Oklahoma City, OK 73104

[2]Department of Anatomy and Life Structure, Juntendo University School of Medicine, Bunkyo-ku, Tokyo 113-8421, Japan

[3]Department of Biological Science and Technology, Graduate school of Industrial Science and Technology, Tokyo University of Science, Noda, Chiba 278-8510, Japan

Abstract

Background—The podocyte slit diaphragm (SD) is an essential component of the selective filtration barrier in the glomerulus. Several structural proteins required for formation and maintenance of SD have been identified; however, molecular mechanisms regulating these proteins are still limited.

Results—Here, we demonstrate that MAGUK p55 subfamily member 5a (Mpp5a)/Nagie oko, a component of the Crb multi-protein complex, was colocalized with an SD-associated protein ZO-1 in the zebrafish pronephric glomerulus. To characterize the function of Mpp5a, zebrafish *mpp5a*^{m520} mutant embryos, which are known to have defects in cardiac and neuronal morphogenesis, were analyzed. These mutants failed to merge the bilateral glomerular primordia and to form the glomerular capillary and mesangium, but the foot processes and SD showed normal appearance. The structural disorganization in the *mpp5a*^{m520} mutant glomerulus was quite similar to that of a *cardiac troponin T2a/tnnt2a/silent heart* knockdown zebrafish, which exhibited circulatory failure due to lack of heart beating.

Conclusions—Mpp5a is not prerequisite to form podocyte slit diaphragm in the pronephric glomerular development in zebrafish. The structural disorganization of the pronephric glomerulus in the *mpp5a*^{m520} mutant is likely to result from circulatory failure, rather than the anomaly of Mpp5a protein in the glomerulus.

Keywords

Glomerulogenesis; Pronephros; Glomerulus; Podocyte; slit diaphragm; *mpp5a*; *nagie oko*; *Danio rerio*

Introduction

The renal glomerulus exhibits a common structural organization among most taxonomic groups in vertebrates, but is obviously adapted to the different homeostatic requirements (Ichimura et al., 2007; Ichimura et al., 2009). Structurally, the glomerulus can be divided into vascular and epithelial regions. The vascular region is the core structure of the

*Correspondence author: Tomoko Obara, Department of Cell Biology, University of Oklahoma Health Science Center, 975, NE 10th St., BRC256, Oklahoma City, OK 73104, Phone: (405) 271-8001 ext. 47035, Fax: (405), 271-3548, tomoko-obara@ouhsc.edu.

$watermark-text
$watermark-text
$watermark-text

$watermark-text

$watermark-text

$watermark-text

glomerulus and consists of the capillary network and the mesangium. The vascular region is surrounded by the epithelial region, a sheet-like structure consisting of podocytes and the glomerular basement membrane (GBM). The vertebrate podocyte is an epithelial cell highly specialized for glomerular filtration. It is composed of three subcellular compartments: a cell body, major processes that extend outward from the cell body, and more distally located foot processes that are spanned by a slit diaphragm (SD) (Mundel and Kriz, 1995; Ichimura et al., 2003; Kriz and Kaissling, 2007). This basic cellular architecture of podocytes is conserved throughout all vertebrates (Youson and McMillan, 1970; Davis et al., 1976; Schwarz and Radke, 1981; Zuasti et al., 1983; Meseguer et al., 1987; Takahashi-Iwanaga, 2002; Møbjerg et al., 2004; Ojéda et al., 2006).

The slit diaphragm is a final element of the filtration barrier that defines size selectivity, and represents a highly modified tight junction (TJ) specialized for ultrafiltration in the glomerulus (Schnabel et al., 1990; Kurihara et al., 1992; Fukasawa et al., 2009). Several TJ-related proteins are commonly found in the SD and SD plaque, which is in direct contact with the inner leaflet of plasma membrane spanning the SD, together with a set of SD-specific proteins including Nephrin, Podocin, and Neph1 (Pavenstadt et al., 2003). Tight junction-related proteins are largely classified into integral-membrane TJ and cytosolic TJ plaque proteins, and these proteins form three kinds of multi-molecular complexes (PAR3-aPKC-PAR6, Crbs-Mpp5/PALS1-PATJ-Lin7, and Scribble-Dlg-Lgl complexes) at the tight junction in mammals (Schneeberger and Lynch, 2004). Some integral-membrane TJ proteins including claudin-7, JAM-2, JAM-4 are localized at the SD, and several TJ plaque proteins (ZO-1, aPKC, cingulin, and so on) are also localized at the SD plaque (Schnabel et al., 1990; Kurihara et al., 1992; Hirabayashi et al., 2005; Hartleben et al., 2008; Fukasawa et al., 2009; Hirose et al., 2009; Huber et al., 2009).

Among TJ proteins, localization and function of the Crbs-Mpp5/PALS1-PATJ-Lin7 complex in podocytes remains unclear. Only Crb2b is known to be localized at the apical membrane of podocytes in the zebrafish pronephric glomerulus, and to contribute to the formation of regular foot processes (Ebarasi et al., 2009). MAGUK p55 subfamily member 5 (Mpp5), a membrane-associated guanylate kinase (MAGUK) protein containing a PDZ domain, can bind to all other components in the complex (Bulgakova and Knust, 2009). Mpp5a/Nagie oko is a zebrafish homologue of mammalian Mpp5/PALS1, and is known to localize at the subapical region of retinal photoreceptor, which corresponds to the typical region containing TJ in other epithelial cell types. Mpp5a plays a crucial role in the formation and maintenance of the retinal cellular patterning in zebrafish (Wei and Malicki, 2002), and is also known to localize at the TJ and regulate morphogenesis in the neuroepithelium and primitive myocardial tube (Rohr et al., 2006; Bit-Avragim et al., 2008; Yang et al., 2009). However, no evidence of Mpp5a localization and function in podocytes has been analyzed.

The pronephros is the simplest and earliest kidney model, which has been used to study embryonic kidney development. This pronephros is a prerequisite for the subsequent formation of mesonephros and metanephros, but their functional unit (the nephron) is organized very similarly (Drummond, 2005; Wingert et al., 2007; Wessely and Obara, 2008). As in fish and amphibians, the zebrafish pronephros is the first kidney to form during embryogenesis and is required to maintain proper osmoregulation (Drummond et al., 1998; Wessely and Obara, 2008; Drummond and Davidson, 2010). Among the different kidney types, the pronephric glomerulus is composed of the same cell types as mammalian glomeruli, including the fenestrated endothelial cells of the capillary tufts and the podocytes with their extensive foot processes and SD (Drummond et al., 1998; Majumdar and Drummond, 2000).

$watermark-text

$watermark-text

$watermark-text

Although some proteins that localize to the SD have been defined, molecular mechanisms that regulate and maintain the SD remain unclear. To address this question, we studied the Mpp5a protein localization in the pronephric glomerulus and analyzed the glomerular structure in zebrafish *mpp5a* mutants. This analysis showed that Mpp5a localized at the podocyte foot processes, *mpp5a* mutants displayed structural disorganization characterized by failure of glomerular primordial fusion and agenesis of glomerular capillary and mesangium. Despite their disorganization, *mpp5a* mutant podocytes still formed regular foot processes with SD. *mpp5a* mutants are also known to exhibit cardiac morphogenesis defects (Rohr et al., 2006). *cardiac troponin T2a/tnnt2a/silent heart* knockdown zebrafish (which lacks a heartbeat) exhibited glomerular disorganization similar to that of *mpp5a* mutants, suggesting that the glomerulus abnormality in the *mpp5a* mutants may be attributable to circulatory insufficiency.

Results

Mpp5a is localized at podocyte foot processes in zebrafish pronephric glomerulus

In the zebrafish pronephros, paired nephron (glomerular and tubular) primordia are formed under the notochord as epithelial flat vesicles at 34 hours post fertilization (hpf) (Drummond et al., 1998). The medial half of the vesicle comprises presumptive podocytes, whereas the lateral half is tubular primordia. At 34 hpf, Mpp5a protein localized to both the medial and lateral halves of nephron primordia (Fig. 1A). Pronephric glomerular primordia fuse to form a single glomerulus concomitantly with capillaries sprouting from the dorsal aorta by 2 days post fertilization (dpf) (Drummond et al., 1998). At 3 dpf, immunoreactivity for Mpp5a was recognized along the glomerular capillary wall in the pronephric glomerulus (white arrowhead in Fig. 1B), which is reminiscent with localization observed for SD-associated proteins such as ZO-1 (Schnabel et al., 1990; Hirabayashi et al., 2005). To further confirm the precise localization of Mpp5a protein, we performed double immunolabeling with anti-Mpp5a and anti-ZO-1 antibodies. The immunoreactivity for ZO-1 was found along the glomerular capillary wall in the pronephric glomerulus (arrowhead in Fig. 1C), similar to the rat metanephric glomerulus (Schnabel et al., 1990). Moreover, Mpp5a and ZO-1 were co-localized at the glomerulus (arrowheads in Fig. 1C–C″). Together these data demonstrate that Mpp5a is localized in the foot processes of zebrafish pronephric podocytes. In addition to Mpp5a localization to the parietal capsule of Bowman's capsule (arrows in Fig. 1C′), pronephric tubule (small arrow in Fig. 1B), and epidermis (yellow arrowheads in Fig. 1A, B), we detected the presence of Mpp5a in the apical junction of the neural tube as previously reported at 34 hpf and 3 dpf (large arrows in Fig. 1A, B).

mpp5a^{m520} mutants display pronephric glomerular disorganization

To determine the role of Mpp5a protein in the zebrafish pronephric glomerulus and filtration barrier, we examined *mpp5a*^{m520} homozygotic mutants. The *mpp5a*^{m520} allele encodes a premature stop codon at residue Arg 546 within the GUK domain (Wei and Malicki, 2002) (Fig. 2).

In the *mpp5a*^{m520} mutant, structural disorganization of the pronephric glomerulus and both pericardial and systemic edema were detected from 2 dpf. In the wild-type sibling, a pair of pronephric glomerular primordia merged with several glomerular capillaries to form a single glomerulus by 2 dpf (Figs. 3A, 3D, 3G, 4A). However, in the 2 dpf *mpp5a*^{m520} mutant, a pair of glomerular primordia retained their epithelial vesicular structure from the previous embryonic stage and did not merge at the midline (Fig. 3B, C). At 3 and 4 dpf, most of the *mpp5a*^{m520} mutants still exhibited unmerged podocyte cell masses (Fig. 3E, F, H, I), which were interposed by an extremely dilated dorsal aorta (Fig. 4B). 3 to 4 dpf wild-type siblings exhibited fine glomerular capillaries and an arborized mesangium within the pronephric

$watermark-text

$watermark-text

$watermark-text

glomerulus (Fig. 4A). In contrast the glomerular primordia in the *mpp5a*^{m520} mutants did not contain fine glomerular capillaries or an arborized mesangium (Fig. 4B).

Expression of *nephrin* mRNA is highly specific in podocytes of the pronephros. In 2 and 3 dpf wild-type siblings, *nephrin* mRNA expresses as a single globular mass in the glomerulus (Fig. 5A, C). In the *mpp5a*^{m520} mutant, the cells expressing *nephrin* (the presumptive glomerular primordia) were arranged in a flattened moustache-like shape in axial section (Fig. 5B, D, E). In the *mpp5a*^{m520} mutant, the *nephrin*-expressing regions were expanded toward the pronephric tubule, similar to *wt1* and *vegf* expression in the *pax2.1/no isthmus* mutant (Majumdar and Drummond, 2000).

Podocyte foot processes and SD were formed in the *mpp5a*^{m520} mutant

The slit diaphragm is a specialized cell-cell junction sometimes described as a highly modified TJ (Schnabel et al., 1990; Kurihara et al., 1992; Fukasawa et al., 2009). Mpp5a is one of the TJ-associated proteins, which have been shown to mediate direct binding to other cell polarity proteins to maintain epithelial integrity and morphogenesis (Wei and Malicki, 2002; Bit-Avragim et al., 2008). The effects of *mpp5a*^{m520} mutation on foot process and filtration barrier formation in the glomerulus were further explored by electron microscopy. In wild-type siblings, foot processes with SD were formed at 3 to 4 dpf, as previously reported (Fig. 6A, B) (Kramer-Zucker et al., 2005; Ferrante et al., 2009). Although the glomerulus structure was disorganized in the *mpp5a*^{m520} mutant (Fig. 6C, D), we noted podocyte foot processes with SD were present and did not demonstrate a flattened or misshapen appearance as seen in the *nephrin* or *podocin* morphants (Kramer-Zucker et al., 2005; Hentschel et al., 2007). However, podocytes in the *mpp5a*^{m520} mutant showed that microvillus-like processes protruded from the apical surface of cell body and primary processes. The adjoined microvillus-like processes formed an SD-like structure (arrows in Fig. 6D).

tnnt2a knockdown induced a disorganized glomerulus similar to that found in *mpp5a*^{m520} mutant

In zebrafish mutants displaying cardiac dysfunction, the paired pronephric glomerular primordia fail to merge into a single glomerulus at 48 hpf. These data suggest that the glomerular disorganization phenotypes may be secondary to the lack of vascular flow associated with cardiac dysfunction (Serluca et al., 2002).

In both *mpp5a* mutants and morphants, heart tube elongation is impaired by the failure of cardiomyocyte cohesion, cell polarity, maintenance of epithelial integrity and cardiac morphogenesis (Rohr et al., 2006). It is thus conceivable that cardiac malformation in *mpp5a* mutants leads to circulatory dysfunction, which in turn negatively impacts glomerular organization. To determine whether glomerular disorganization was a phenotype consistently associated with circulatory failure, we examined glomerular organization and podocyte ultrastructure in *cardiac troponin T2a/tnnt2a/silent heart-ATG* morphants, which displayed complete cardiac arrest throughout their survival period (Sehnert et al., 2002). In 2 dpf *tnnt2a-ATG* morphants, the paired glomerular primordia retained their prior epithelial vesicular structure and remained unmerged at the midline (Fig. 7B), as seen in the *mpp5a*^{m520} mutant (Figs. 3B, C, 5B), and other mutants with circulatory failure (Serluca et al., 2002). In 3 and 4 dpf, an extremely dilated dorsal aorta was interposed between the glomerular primordial, which still remained unmerged (Figs. 4C, 7D, F). The glomerular primordia did not show any evidence of fine glomerular capillaries or an arborized mesangium, which were readily observed in the normal glomerulus by this stage (Fig. 4C). The *nephrin*-expressing regions exhibited a moustache-like shape that expanded toward the pronephric tubule, as was the case for the *mpp5a*^{m520} mutant (Fig. 7H, J). Podocytes formed

$watermark-text

$watermark-text

$watermark-text

regular foot processes with SD (Fig. 6E, F). Many microvillus-like processes interbridged to form SD-like structures, which protruded from the apical surface of the cell body and extended primary processes into the Bowman's space (Fig. 6F). Therefore, a series of parallel glomerular phenotypes was observed in the *mpp5a*^{m520} mutant and *tnnt2a-ATG* morphant.

Discussion

Mpp5a is an SD-associated component but is not essential for the formation of foot processes and the SD in zebrafish pronephric podocytes

Several kinds of TJ-plaque proteins are localized to podocyte foot processes and involved in the formation of multi-molecular complexes at the SD plaques of these cells (Kriz and Kaissling, 2007; Fukasawa et al., 2009). ZO-1 is one example of TJ-plaque proteins that are localized at the SD plaque in mammals. Immunoreactivity for ZO-1 is recognized along the glomerular capillary wall as along a continuous tortuous line within the rat metanephric glomerulus (Schnabel et al., 1990). In the zebrafish pronephric glomerulus, ZO-1 localization occurs in a pattern similar to the mammalian metanephros, indicating that it is also localized at the SD plaque of zebrafish pronephric podocytes. Moreover, the colocalization of Mpp5a and ZO-1 suggests that Mpp5a is highly likely to be localized at the SD plaque of the podocyte foot processes.

The *mpp5a*^{m520} mutation causes a C-terminal truncation of the GUK domain, with the result that Mpp5a^{m520} is expressed at two- to three-fold lower levels than wild-type Mpp5a on immunoblot analysis (Wei and Malicki, 2002). However, we observed neither the effacement of foot processes nor the loss of SD in the *mpp5a*^{m520} mutant at 4 dpf. These results suggest that even though Mpp5a is localized to the SD plaque, it is not required for the initial formation of foot processes with SD in the zebrafish pronephric glomerulus.

PAR6-PAR3-aPKC regulates apicobasal epithelial polarity in mouse podocytes, and PAR3 and PAR6 directly bind to SD core components Nephrin and Neph1, respectively (Hartleben et al., 2008; Hirose et al., 2009; Huber et al., 2009). Podocyte-specific deletion of aPKC in mice results in foot process effacement, proteinuria, and focal segmental glomerulosclerosis, although regular foot processes with SD are initially formed during glomerular development (Hirose et al., 2009; Huber et al., 2009). Based on these findings, aPKC is not essential to the initial formation of SD, but is crucial for the maintenance and structural integrity of SD (Hirose et al., 2009). Mpp5a is not also a prerequisite to SD formation; however, it may be involved in the maintenance of SD integrity, as is the case for aPKC. To directly examine this possibility, we would need a podocyte specific *mpp5a* knockdown in zebrafish, since *mpp5a* mutants and *mpp5a-ATG* morphants are known to display severe phenotypes in heart and central nervous system, and die at the early phase after hatching (Wei and Malicki, 2002; Rohr et al., 2006). Moreover, zebrafish has another mammalian Mpp5 homologue, Mpp5b/Ponli, whose expression is restricted to the photoreceptor layer in eyes, unlike Mpp5a (Zou et al., 2010). Mpp5b thus has the potential to compensate for the functional failure of Mpp5a^{m520}.

Structural disorganization of pronephric glomerulus is associated with circulatory failure in multiple mutants

The pronephric glomerulus in the *mpp5a*^{m520} mutant displayed three kinds of structural anomalies: unmerged glomerular primordia, glomerular capillary agenesis and mesangial agenesis. Similar anomalies have been recognized in the cardiac specific troponin gene *tnnt2a* knockdown in zebrafish, which has severe circulatory failure due to the lack of myocardial contraction (Sehnert et al., 2002). Previous work showed that the midline fusion

$watermark-text

$watermark-text

$watermark-text

of pronephric glomerular primordia in zebrafish is dependent on the expression of matrix metalloproteinase-2. This enzyme is induced by hemodynamic forces including shear stress that arise during blood flow and/or stretch forces associated with blood pressure (Serluca et al., 2002). However, the fusion of glomerular primordia is not essential to form the glomerular capillary tuft in the pronephros, since the organized glomerular capillary tuft is seen in several kinds of teleost fish (including medaka *Oryzias latipes*) in which the paired pronephric glomeruli remain separated (Fedorova et al., 2008; Ichimura et al., 2012). In general, hemodynamic forces are known to be a crucial trigger to form the mature vasculature (Lucitti et al., 2007; Culver and Dickinson, 2010; Jones, 2011), and thus it is conceivable that the agenesis of glomerular capillary in the *tnnt2a-ATG* morphants is directly associated with impairment of blood circulation. The *mpp5a*^{m520} mutant is known to have incomplete heart tube elongation coupled with the failure of myocardial cell to correctly expand in size (Rohr et al., 2006). Therefore, a logical explanation for the structural disorganization of the pronephric glomerulus in the *mpp5a*^{m520} mutants is that circulatory failure alters the local environment in a way that impacts morphogenesis, rather than disorganization being directly due to anomaly of Mpp5a protein in the glomerulus. However, as mentioned above, Mpp5a may be involved in the maintenance of SD integrity in the late stage of development, as is the case for aPKC.

Furthermore, by phenotypic analysis of selected zebrafish mutants and morphants, we recognized that circulatory failure due to cardiac defects was consistently correlated with abnormal pronephric glomerular architecture during development. Since zebrafish *tnnt2a* is not expressed in the developing glomerulus or surrounding cells, the glomerular defects in morphants are unlikely to directly arise via *tnnt2a* depletion in the embryonic kidney.

Microvillus-like processes with SD-like structure in podocytes

The pronephric podocytes of the *mpp5a*^{m520} mutant displayed a number of microvillus-like processes, which were connected to each other by an SD-like structure. These unique processes are also found in mutants or morphants of genes expressed in podocytes, including *EPB41L5/mosaic eye (moe)*, encoding a FERM domain-containing actin-binding protein, and *myh9*, encoding a non-muscle myosin heavy chain IIA (Kramer-Zucker et al., 2005; Müller et al., 2011). However, the appearance of the SD-like structure is most likely not directly due to deficiency or anomaly of these proteins, since the same structure was found in the *tnnt2a* knockdown zebrafish and *tnnt2a* is exclusively expressed in the cardiomyocytes. The *mpp5a* mutants and *myh9* morphants exhibit defects of the heart tube elongation and heart folding, respectively (Rohr et al., 2006; Müller et al., 2011), implying that circulatory failure may also be involved in the formation of the microvillus-like processes with SD-like structure.

Such microvillus-like processes have not been reported yet in higher vertebrates including rodents and human, but are found at mesonephric mature podocytes in some lower vertebrates including Atlantic hagfish, *Myxine glutinosa* (Kühn et al., 1980) and Japanese red-bellied newt, *Cynops pyrrhogaster* (our unpublished data). Furthermore, the podocyte-like cells of some invertebrates (amphioxus, echinoderm, and so on) possess a solitary cilium surrounded by 7 to 9 microvillus-like processes cross-linked by SD-like structure on their apical surface (Ruppert et al., 2003; Schmidt-Rhaesa, 2007). The microvillus-like processes are formed under normal physiological condition in these animal species, but their functional significance remains largely unknown.

$watermark-text

$watermark-text

$watermark-text

Experimental Procedures

Fish maintenance and stocks

Heterozygous *mpp5a*^{m520} zebrafish mutants (Wei and Malicki, 2002) were maintained at 28.5°C under a 14-hr light/10-hr dark cycle (Westerfield, 2000). Embryos were kept at 28.5°C in 0.5X E2 egg medium (7.5 mM NaCl, 0.25 mM KCl, 0.5 mM $CaCl_2$, 0.5 mM $MgSO_4$, 0.075 mM KH_2PO_4, 0.025 mM Na_2HPO_4, 0.35 mM $NaHCO_3$, 0.01% methylene blue). To suppress pigmentation of zebrafish embryos, 0.0045% 1-Phenyl-2-thiourea (Sigma-Aldrich) was added to 0.5X E2 egg medium. Embryos were collected according to the staging method described by Kimmel et al. (1995). All animal experiments were performed in strict accordance with the recommendation in the Guide for the Care and Use of Laboratory Animals of the National Institutes of Health, and were covered by protocols approved from the Institutional Animal Care and Use Committee of the University of Oklahoma Health Science Center (IACUC protocol #12-033 to TO). (Kimmel et al., 1995)

Morpholino injection

A translational-blocking antisense-morpholino oligonucleotide (MO) designed to target the 5′UTR of *tnnt2a (tnnt2a-ATGMO*: 5′-CAT GTT TGC TCT GAT CTG ACA CGC A-3′) (Sehnert et al., 2002) was purchased from Gene Tools LCC. A volume of 4.6 nl in a concentration of 0.1 mM *tnnt2a-ATGMO* was injected at one- or two-cell stage using a Nanoliter2000 microinjector (World Precision Instruments). A stable non-contractile heart phenotype was recognized in ~98% of injected larvae at 2 and 3 dpf. Morphants without obvious motility defects and lacking blood circulation (with pericardial edema) were used for the analysis.

Histological analysis

Embryos were fixed with histology fixative (1.5% glutaraldehyde, 4% paraformaldehyde, 3% sucrose in 0.1 mM phosphate buffer (PB, pH 7.3)) overnight at 4°C, dehydrated by graded series of methanol and embedded in JB4 resin (Polysciences, Inc.). 4 μm-thick sections were cut by a RN2255 microtome (Leica) and stained with Harris hematoxylin and special eosin II (BBC Biochemical). After being mounted in Poly-Mount (Polysciences, Inc.), the stained sections were imaged with a Provis AX-70 microscope (Olympus) equipped with a RETIGA EXi digital camera (QImaging).

In situ hybridization

Zebrafish nephrin cDNA template was obtained from pCR-BluntII-TOPO-zebrafish *nephrin* plasmid linearized by *NotI* as described in Kramer-Zucker et al. (2005). Digoxigenin-labeled anti-sense *nephrin* RNA probe was synthesized using *SP6* RNA polymerase (New England BioLabs) and DIG-RNA labeling (Roche) according to the manufacturer's instructions. Embryos were fixed in 4% PFA, 0.1% Tween 20 in PBS for 2 h at RT and changed to 100% methanol and stored at −20°C. Whole mount *in situ* hybridization was performed as described previously (Hauptmann and Gerster, 2000). Alkaline phosphatase-conjugated anti-digoxigenin (Roche) was used to localize the probes. NBT/BCIP (Roche) was used as the chromogenic substrate to produce the blue staining. After color development, samples were dehydrated with graded series of methanol and embedded in JB4 resin. Five to seven μm-thick sections were cut by a RN2255 microtome and counter-stained with special eosin II (BBC Biochemical). After mounted in Poly-Mount, the stained sections were photographed on a Provis AX-70 microscope equipped with a RETIGA EXi digital camera.

$watermark-text

$watermark-text

$watermark-text

Antibodies and whole mount immunohistochemistry

Rabbit polyclonal anti-zebrafish Mpp5a antibody (a kind gift from Dr. X. Wei) was raised against the glutathione S-transferase fusion protein with the N-terminal portion of zebrafish Mpp5a (27–280 amino acids) (Wei and Malicki, 2002). Mouse monoclonal anti-rat ZO-1 (a kind gift from Drs. S. Tsukita and S. Tsukita) was raised against the fraction rich in adherence junction obtained from rat liver (Itoh et al., 1991). Whole mount immunohistochemistry was performed as described previously (Bubenshchikova et al., 2012). In brief, embryos were fixed with Dent's fixative (20% DMSO and 80% methanol) overnight at 4°C. Fixed samples were washed with PBS containing 0.5% Triton X-100 (PBSTx), blocked with blocking solution (PBS containing 0.5% Triton X-100, 10% normal goat serum, and 1% DMSO) and incubated overnight with the anti-Mpp5a antibody (working dilution 1:100) with incubation buffer (PBS containing 0.5% Triton X-100, 2% normal goat serum, and 1% DMSO). After washing with PBSTx, the samples were incubated with Alexa-Fluor488-conjugated goat anti-rabbit IgG (H+L) (Jackson ImmunoResearch Laboratories) diluted with the incubation solution (1:1000) for 2 h at RT. Some samples were subsequently incubated with anti-ZO-1 antibody with incubation buffer (1:100) for overnight at 4°C, and then with Alexa-Fluor568-conjugated goat anti-rabbit IgG (H+L) (Jackson ImmunoResearch Laboratories) with the incubation solution (1:1000) for 2 h at RT. Stained samples were dehydrated with a graded series of methanol, embedded in JB4 resin, and cut into 10 μm-thick sections. The sections were imaged with a FV-1000 confocal laser scanning microscope (Olympus).

Transmission electron microscopy

Embryos were immersed in histology fixative for overnight at 4°C. The samples were immersed in 1% OsO_4 in 0.1 M PB for 1 h, and then dehydrated with a graded series of acetone, and were embedded in Epon-Araldite resin (Electron Microscopy Sciences). Ultrathin silver-gold sections were produced with an ultra 45° diamond knife (Diatome), and were transferred to copper grids (50 mesh), which had been coated with Formvar membrane. The sections were then stained with uranyl acetate and lead citrate, and imaged on an H-7600 transmission electron microscope (Hitachi High Technologies Inc.) equipped with a Kodak 2Kx2K digital camera (Kodak).

Acknowledgments

The authors thank Drs. Deborah Garrity, and Hiroyuki Matsumoto for helpful criticism and comments on the manuscript. Dr. Xiangyun Wei generously provided the anti-Mpp5a antibody and *mpp5a*^{m520} mutants. The anti-ZO-1 antibody was provided from Drs. Shoichiro Tsukita and Sachiko Tsukita. T.O. acknowledges financial support from the University of Oklahoma Health Science Center (OUHSC). K.I. was supported by Grants-in-Aid for Scientific Research from the Ministry of Education, Culture, Sports, Science and Technology of Japan (No. 23590226). T.O. was supported by NIH grants R21-DK069604, and R01-DK078209. This work is supported in part by the Diabetes Histology and Image Acquisition and Analysis Core Facility at OUHSC (NIH: COBRE-1P20RR024215) and the Imaging Core Facility at Oklahoma Medical Research Foundation.

References

Bit-Avragim N, Hellwig N, Rudolph F, Munson C, Stainier DY, Abdelilah-Seyfried S. Divergent polarization mechanisms during vertebrate epithelial development mediated by the Crumbs complex protein Nagie oko. J Cell Sci. 2008; 121(Pt 15):2503–2510. [PubMed: 18628301]

Bubenshchikova E, Ichimura K, Fukuyo Y, Powell R, Hsu C, Morrical SO, Sedor JR, Sakai T, Obara T. Wtip and Vangl2 are required for mitotic spindle orientation and cloaca morphogenesis. Biology Open. 2012; 1:588–596.

Bulgakova NA, Knust E. The Crumbs complex: from epithelial-cell polarity to retinal degeneration. J Cell Sci. 2009; 122(Pt 15):2587–2596. [PubMed: 19625503]

$watermark-text

$watermark-text

$watermark-text

Culver JC, Dickinson ME. The effects of hemodynamic force on embryonic development. Microcirculation. 2010; 17(3):164–178. [PubMed: 20374481]

Davis LE, Schmidt-Nielsen B, Stolte H. Anatomy and ultrastructure of the excretory system of the lizard, *Sceloporus cyanogenys*. J Morphol. 1976; 149(3):279–326. [PubMed: 957443]

Drummond IA. Kidney development and disease in the zebrafish. J Am Soc Nephrol. 2005; 16(2): 299–304. [PubMed: 15647335]

Drummond IA, Davidson AJ. Zebrafish kidney development. Methods Cell Biol. 2010; 100:233–260. [PubMed: 21111220]

Drummond IA, Majumdar A, Hentschel H, Elger M, Solnica-Krezel L, Schier AF, Neuhauss SC, Stemple DL, Zwartkruis F, Rangini Z, et al. Early development of the zebrafish pronephros and analysis of mutations affecting pronephric function. Development. 1998; 125(23):4655–4667. [PubMed: 9806915]

Ebarasi L, He L, Hultenby K, Takemoto M, Betsholtz C, Tryggvason K, Majumdar A. A reverse genetic screen in the zebrafish identifies crb2b as a regulator of the glomerular filtration barrier. Dev Biol. 2009; 334(1):1–9. [PubMed: 19393641]

Fedorova S, Miyamoto R, Harada T, Isogai S, Hashimoto H, Ozato K, Wakamatsu Y. Renal glomerulogenesis in medaka fish, Oryzias latipes. Dev Dyn. 2008; 237(9):2342–2352. [PubMed: 18729228]

Ferrante MI, Romio L, Castro S, Collins JE, Goulding DA, Stemple DL, Woolf AS, Wilson SW. Convergent extension movements and ciliary function are mediated by ofd1, a zebrafish orthologue of the human oral-facial-digital type 1 syndrome gene. Hum Mol Genet. 2009; 18(2): 289–303. [PubMed: 18971206]

Fukasawa H, Bornheimer S, Kudlicka K, Farquhar MG. Slit diaphragms contain tight junction proteins. J Am Soc Nephrol. 2009; 20(7):1491–1503. [PubMed: 19478094]

Hartleben B, Schweizer H, Lubben P, Bartram MP, Moller CC, Herr R, Wei C, Neumann-Haefelin E, Schermer B, Zentgraf H, et al. Neph-Nephrin proteins bind the Par3-Par6-atypical protein kinase C (aPKC) complex to regulate podocyte cell polarity. J Biol Chem. 2008; 283(34):23033–23038. [PubMed: 18562307]

Hauptmann G, Gerster T. Multicolor whole-mount in situ hybridization. Methods Mol Biol. 2000; 137:139–148. [PubMed: 10948532]

Hentschel DM, Mengel M, Boehme L, Liebsch F, Albertin C, Bonventre JV, Haller H, Schiffer M. Rapid screening of glomerular slit diaphragm integrity in larval zebrafish. Am J Physiol Renal Physiol. 2007; 293(5):F1746–F1750. [PubMed: 17699558]

Hirabayashi S, Mori H, Kansaku A, Kurihara H, Sakai T, Shimizu F, Kawachi H, Hata Y. MAGI-1 is a component of the glomerular slit diaphragm that is tightly associated with nephrin. Lab Invest. 2005; 85(12):1528–1543. [PubMed: 16155592]

Hirose T, Satoh D, Kurihara H, Kusaka C, Hirose H, Akimoto K, Matsusaka T, Ichikawa I, Noda T, Ohno S. An essential role of the universal polarity protein, aPKClambda, on the maintenance of podocyte slit diaphragms. PLoS One. 2009; 4(1):e4194. [PubMed: 19142224]

Huber TB, Hartleben B, Winkelmann K, Schneider L, Becker JU, Leitges M, Walz G, Haller H, Schiffer M. Loss of podocyte aPKClambda/iota causes polarity defects and nephrotic syndrome. J Am Soc Nephrol. 2009; 20(4):798–806. [PubMed: 19279126]

Ichimura K, Bubenshchikova E, Powell R, Fukuyo Y, Nakamura T, Tran U, Oda S, Tanaka M, Wessely O, Kurihara H, et al. A comparative analysis of glomerulus development in the pronephros of medaka and zebrafish. PLoS One. 2012; 7(9):e45286. [PubMed: 23028906]

Ichimura K, Kurihara H, Sakai T. Actin filament organization of foot processes in rat podocytes. J Histochem Cytochem. 2003; 51(12):1589–1600. [PubMed: 14623927]

Ichimura K, Kurihara H, Sakai T. Actin filament organization of foot processes in vertebrate glomerular podocytes. Cell Tissue Res. 2007; 329(3):541–557. [PubMed: 17605050]

Ichimura K, Kurihara H, Sakai T. Beta-cytoplasmic actin localization in vertebrate glomerular podocytes. Arch Histol Cytol. 2009; 72(3):165–174. [PubMed: 20513979]

Itoh M, Yonemura S, Nagafuchi A, Tsukita S. A 220-kD undercoat-constitutive protein: its specific localization at cadherin-based cell-cell adhesion sites. J Cell Biol. 1991; 115(5):1449–1462. [PubMed: 1955485]

$watermark-text

$watermark-text

$watermark-text

Jones EA. The initiation of blood flow and flow induced events in early vascular development. Semin Cell Dev Biol. 2011; 22(9):1028–1035. [PubMed: 22001248]

Kühn KW, Luciano L, Stolte H, Reale E. Cell junctions of the glomerular epithelium in a very early vertebrate (Myxine glutinosa). Contrib Nephrol. 1980; 19:9–14. [PubMed: 7379549]

Kimmel CB, Ballard WW, Kimmel SR, Ullmann B, Schilling TF. Stages of embryonic development of the zebrafish. Dev Dyn. 1995; 203(3):253–310. [PubMed: 8589427]

Kramer-Zucker AG, Wiessner S, Jensen AM, Drummond IA. Organization of the pronephric filtration apparatus in zebrafish requires Nephrin, Podocin and the FERM domain protein Mosaic eyes. Dev Biol. 2005; 285(2):316–329. [PubMed: 16102746]

Kriz, W.; Kaissling, B. Structural Organization of the Mammalian Kidney. In: Alpern, RJ.; Hebert, SC., editors. Seldin and Giebisch's The Kidney -physiology and pathophysiology-. Vol. vol. 1. Academic Press; 2007.

Kurihara H, Anderson JM, Farquhar MG. Diversity among tight junctions in rat kidney: glomerular slit diaphragms and endothelial junctions express only one isoform of the tight junction protein ZO-1. Proc Natl Acad Sci U S A. 1992; 89(15):7075–7079. [PubMed: 1496002]

Lucitti JL, Jones EA, Huang C, Chen J, Fraser SE, Dickinson ME. Vascular remodeling of the mouse yolk sac requires hemodynamic force. Development. 2007; 134(18):3317–3326. [PubMed: 17720695]

Møbjerg N, Jespersen Å, Wilkinson M. Morphology of the kidney in the West African caecilian, *Geotrypetes seraphini* (Amphibia, Gymnophiona, Caeciliidae). J Morphol. 2004; 262(2):583–607. [PubMed: 15376276]

Müller T, Rumpel E, Hradetzky S, Bollig F, Wegner H, Blumenthal A, Greinacher A, Endlich K, Endlich N. Non-muscle myosin IIA is required for the development of the zebrafish glomerulus. Kidney Int. 2011; 80(10):1055–1063. [PubMed: 21849970]

Majumdar A, Drummond IA. The zebrafish floating head mutant demonstrates podocytes play an important role in directing glomerular differentiation. Dev Biol. 2000; 222(1):147–157. [PubMed: 10885753]

Meseguer J, Garcia Ayala A, Agulleiro B. Ultrastructure of the nephron of freshwater turtles, *Pseudemys scripta elegans* and *Mauremys caspica*. Cell Tissue Res. 1987; 248(2):381–391. [PubMed: 3581151]

Mundel P, Kriz W. Structure and function of podocytes: an update. Anat Embryol (Berl). 1995; 192(5):385–397. [PubMed: 8546330]

Ojéda JL, Icardo JM, Wong WP, Ip YK. Microanatomy and ultrastructure of the kidney of the African lungfish *Protopterus dolloi*. Anat Rec Part A. 2006; 288A(6):609–625.

Pavenstadt H, Kriz W, Kretzler M. Cell biology of the glomerular podocyte. Physiol Rev. 2003; 83(1): 253–307. [PubMed: 12506131]

Rohr S, Bit-Avragim N, Abdelilah-Seyfried S. Heart and soul/PRKCi and nagie oko/Mpp5 regulate myocardial coherence and remodeling during cardiac morphogenesis. Development. 2006; 133(1): 107–115. [PubMed: 16319113]

Ruppert, E.; Fox, R.; Barnes, R. Invertebrate zoology. Belmont: Thomson Learning; 2003.

Schmidt-Rhaesa, A. The evolution of organ systems. New York: Oxford University Press; 2007. Excreatory system.

Schnabel E, Anderson JM, Farquhar MG. The tight junction protein ZO-1 is concentrated along slit diaphragms of the glomerular epithelium. J Cell Biol. 1990; 111(3):1255–1263. [PubMed: 2202736]

Schneeberger EE, Lynch RD. The tight junction: a multifunctional complex. Am J Physiol Cell Physiol. 2004; 286(6):C1213–C1228. [PubMed: 15151915]

Schwarz R, Radke B. Microscopic study of the effect of varied high concentrations of fluid on the morphology of renal corpuscles of the chicken (*Gallus domesticus*). Anat Histol Embryol. 1981; 10(2):167–179. (in Germany with English abstract). [PubMed: 6455935]

Sehnert AJ, Huq A, Weinstein BM, Walker C, Fishman M, Stainier DY. Cardiac troponin T is essential in sarcomere assembly and cardiac contractility. Nat Genet. 2002; 31(1):106–110. [PubMed: 11967535]

Serluca FC, Drummond IA, Fishman MC. Endothelial signaling in kidney morphogenesis: a role for hemodynamic forces. Curr Biol. 2002; 12(6):492–497. [PubMed: 11909536]

Takahashi-Iwanaga H. Comparative anatomy of the podocyte: A scanning electron microscopic study. Microsc Res Tech. 2002; 57(4):196–202. [PubMed: 12012383]

Wei X, Malicki J. nagie oko, encoding a MAGUK-family protein, is essential for cellular patterning of the retina. Nat Genet. 2002; 31(2):150–157. [PubMed: 11992120]

Wessely O, Obara T. Fish and frogs: models for vertebrate cilia signaling. Front Biosci. 2008; 13:1866–1880. [PubMed: 17981674]

Westerfield, M. The Zebrafish Book: a Guide for the Laboratory Use of Zebrafish. Eugene, OR: 2000.

Wingert RA, Selleck R, Yu J, Song HD, Chen Z, Song A, Zhou Y, Thisse B, Thisse C, McMahon AP, et al. The cdx genes and retinoic acid control the positioning and segmentation of the zebrafish pronephros. PLoS Genet. 2007; 3(10):1922–1938. [PubMed: 17953490]

Yang X, Zou J, Hyde DR, Davidson LA, Wei X. Stepwise maturation of apicobasal polarity of the neuroepithelium is essential for vertebrate neurulation. J Neurosci. 2009; 29(37):11426–11440. [PubMed: 19759292]

Youson JH, McMillan DB. The opisthonephric kidney of the sea lamprey of the Great Lakes, *Petromyzon marinus* L.I. The renal corpuscle. Am J Anat. 1970; 127(3):207–213. [PubMed: 5436821]

Zou J, Yang X, Wei X. Restricted localization of ponli, a novel zebrafish MAGUK-family protein, to the inner segment interface areas between green, red, and blue cones. Invest Ophthalmol Vis Sci. 2010; 51(3):1738–1746. [PubMed: 19834027]

Zuasti A, Agulleiro B, Hernandez F. Ultrastructure of the kidney of the marine teleost *Sparus auratus*: the renal corpuscle and the tubular nephron. Cell Tissue Res. 1983; 228(1):99–106. [PubMed: 6831529]

$watermark-text

$watermark-text

$watermark-text

$watermark-text

$watermark-text

$watermark-text

Bullet points

- Mpp5a is localized at the podocyte foot process in the zebrafish pronephric glomerulus.
- Zebrafish *mpp5a*^{m520} mutants display structural disorganization of the pronephric glomerulus including glomerular capillary agenesis, but regular foot processes with slit a diaphragm were formed.
- Mpp5a is not prerequisite to form podocyte slit diaphragm in the pronephric glomerular development in zebrafish.

$watermark-text
$watermark-text
$watermark-text

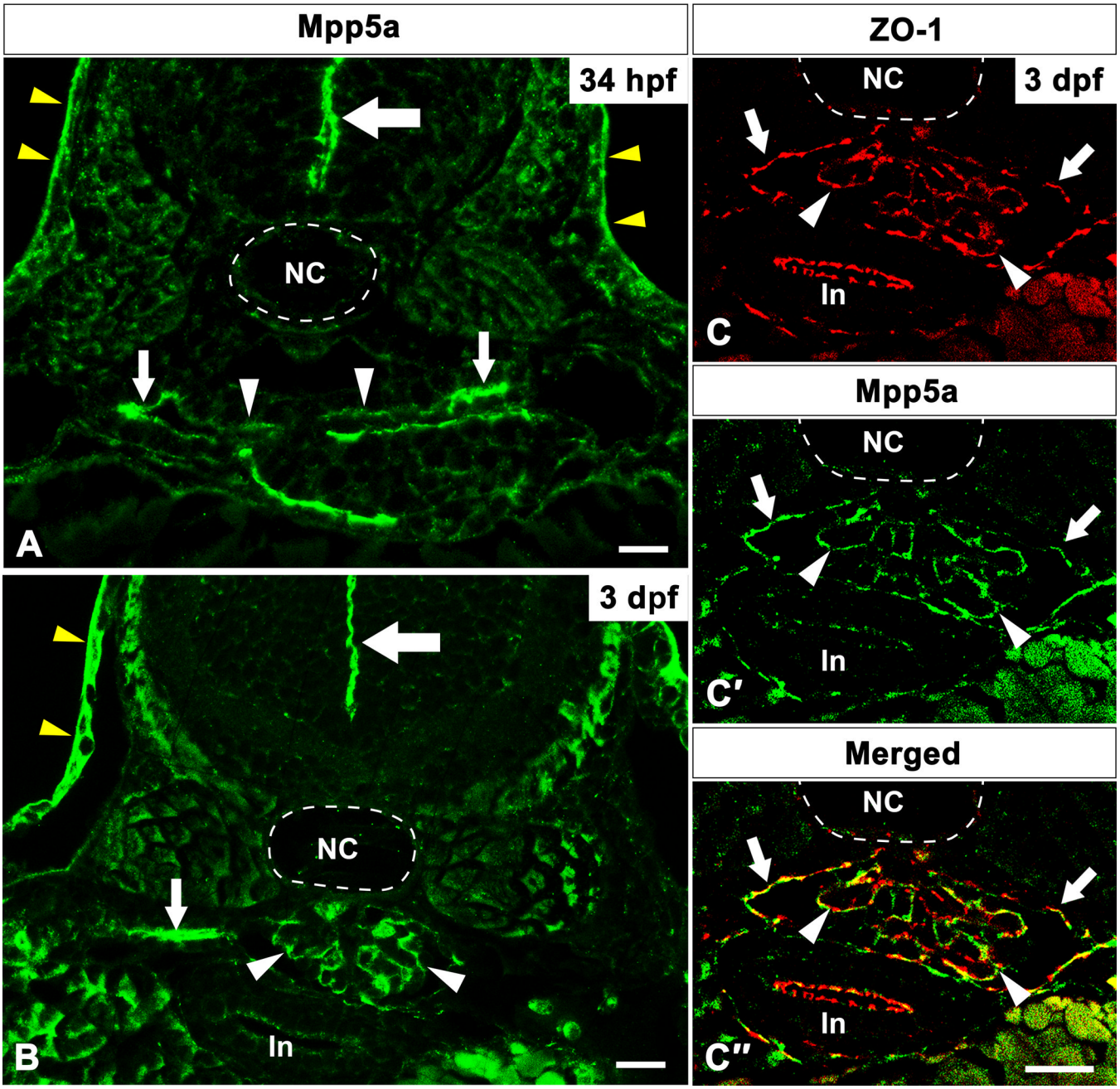

Figure 1.

Mpp5a protein localization in zebrafish pronephric glomerulus. Immunoreactivity for Mpp5a protein is found in both medial and lateral half of nephron primordia at 34 hpf (arrowhead and small arrows in A). At 3 dpf, the signal for Mpp5a is found along the glomerular capillary wall as a tortuous line (arrowhead in B), in addition to the pronephric tubule (small arrows in B). Mpp5a signal is also found at the position of apical tight junction of neural tube (large arrows in A, B). In 3 dpf, immunoreactivity for ZO-1 (red) and Mpp5a (green) are colocalized within the glomerulus (arrowheads in C–C″). Mpp5a signal is also found at parietal epithelium of Bowman's capsule (arrows in C–C″). In, intestine; NC, notochord. Scale bar = 10 μm.

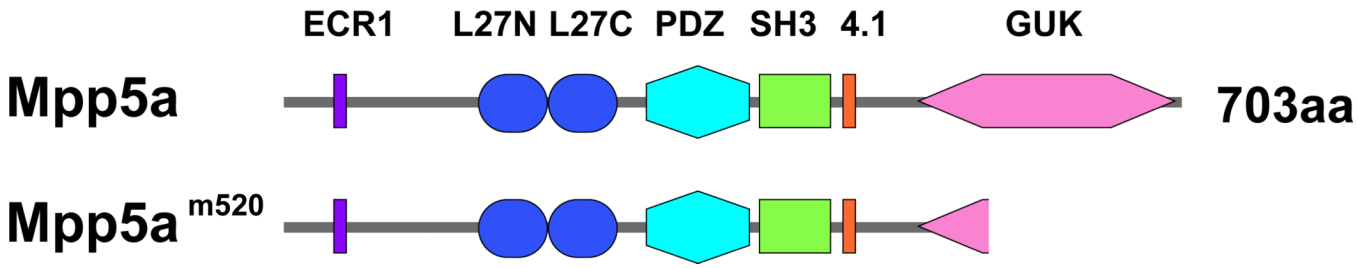

Figure 2.

mpp5a^{m520} mutants partially lacks the N-terminal GUK domain of the Mpp5a protein. Mpp5a is a membrane-associated guanylate kinase protein which contains an evolutionary conserved region 1 (ECR1), a bipartite L27 domain (L27N, L27C), PDZ, SH3, 4.1, and guanylate kinase (GUK) domains. The *mpp5a*^{m520} allele carries single base pair substitution that introduces stop codons within the GUK domain, causing a C-terminal truncation of the GUK domain.

$watermark-text
$watermark-text
$watermark-text

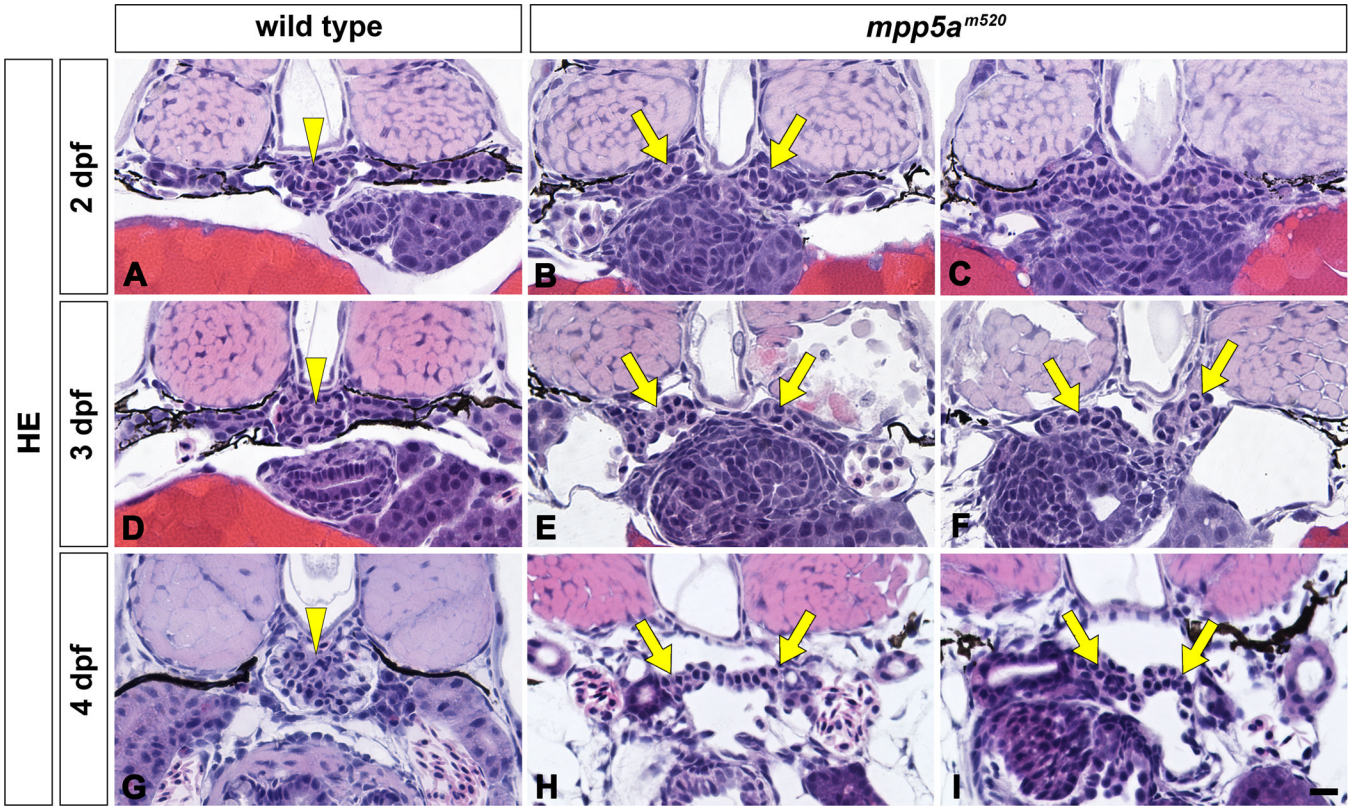

Figure 3.

mpp5a^{m520} mutant displays structural disorganization of pronephric glomerulus. Pronephric glomerular structure is shown by hematoxylin-eosin stained JB-4 section at 2 dpf (A–C), 3 dpf (D–F), and 4 dpf (G–I). In wild type siblings, a pair of glomerular primordia has merged to form a single glomerulus (arrowheads) beneath the notochord at 2 dpf (A), 3 dpf (D), and 4 dpf (G). In 2 dpf *mpp5a*^{m520} mutants, a pair of glomerular primordia retains epithelial vesicular structure and does not merge beneath the notochord (arrows in B, C). At 3 and 4 dpf *mpp5a*^{m520} mutants exhibited still two separated podocyte masses (arrows in E, F, H, I). Scale bar = 10 μm.

$watermark-text
$watermark-text
$watermark-text

$watermark-text
$watermark-text
$watermark-text

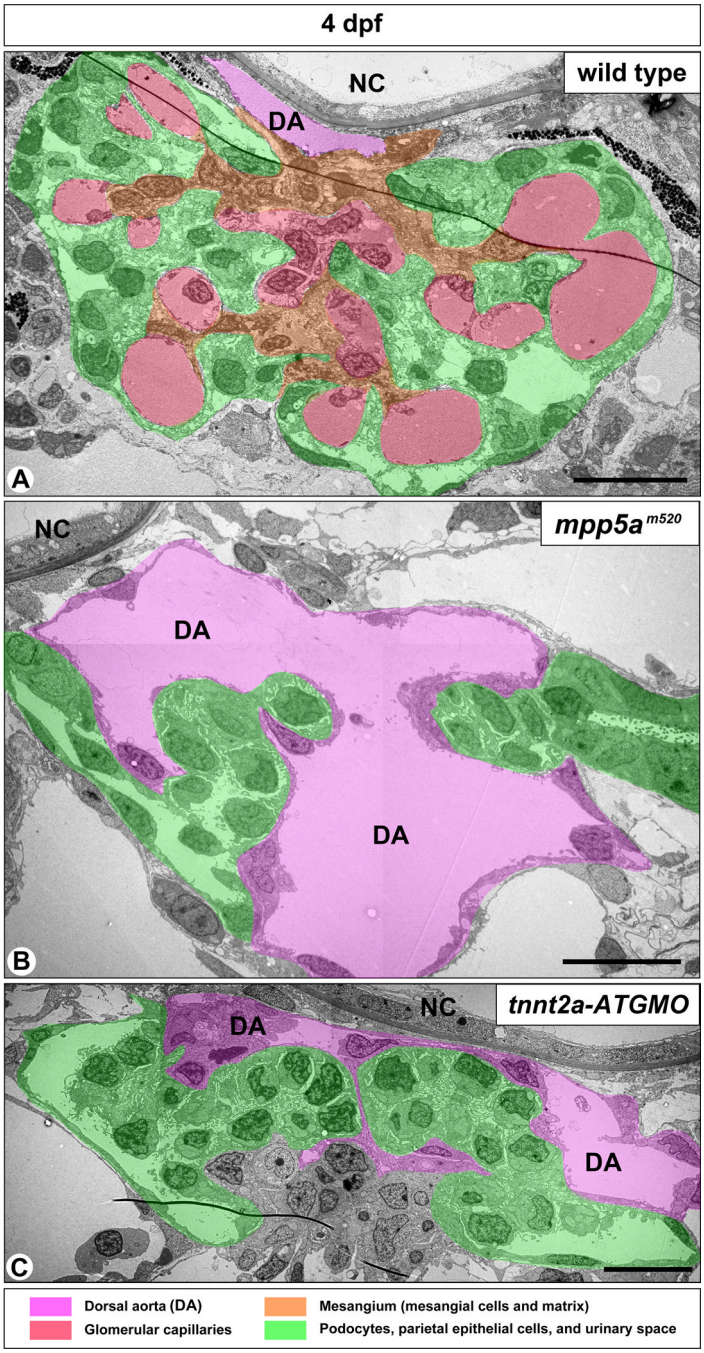

Figure 4.

mpp5a^{m520} mutants and *tnnt2a-ATG* morphants display similar structural disorganization of pronephric glomerulus. (A) In 4 dpf wild-type embryos, the pronephric glomerulus contains several glomerular capillaries together with mesangium, which is arborized in shape. Podocytes and GBM cover the glomerular capillaries and mesangium *en bloc*. In both 4 dpf *mpp5a*^{m520} mutants (B) and *tnnt2a-ATG* morphants (C), the extremely dilated dorsal aorta (DA) lies between a pair of glomerular primordia, which do not contain any fine glomerular capillaries or mesangium. NC, notochord. Scale bar = 500 nm.

$watermark-text
$watermark-text
$watermark-text

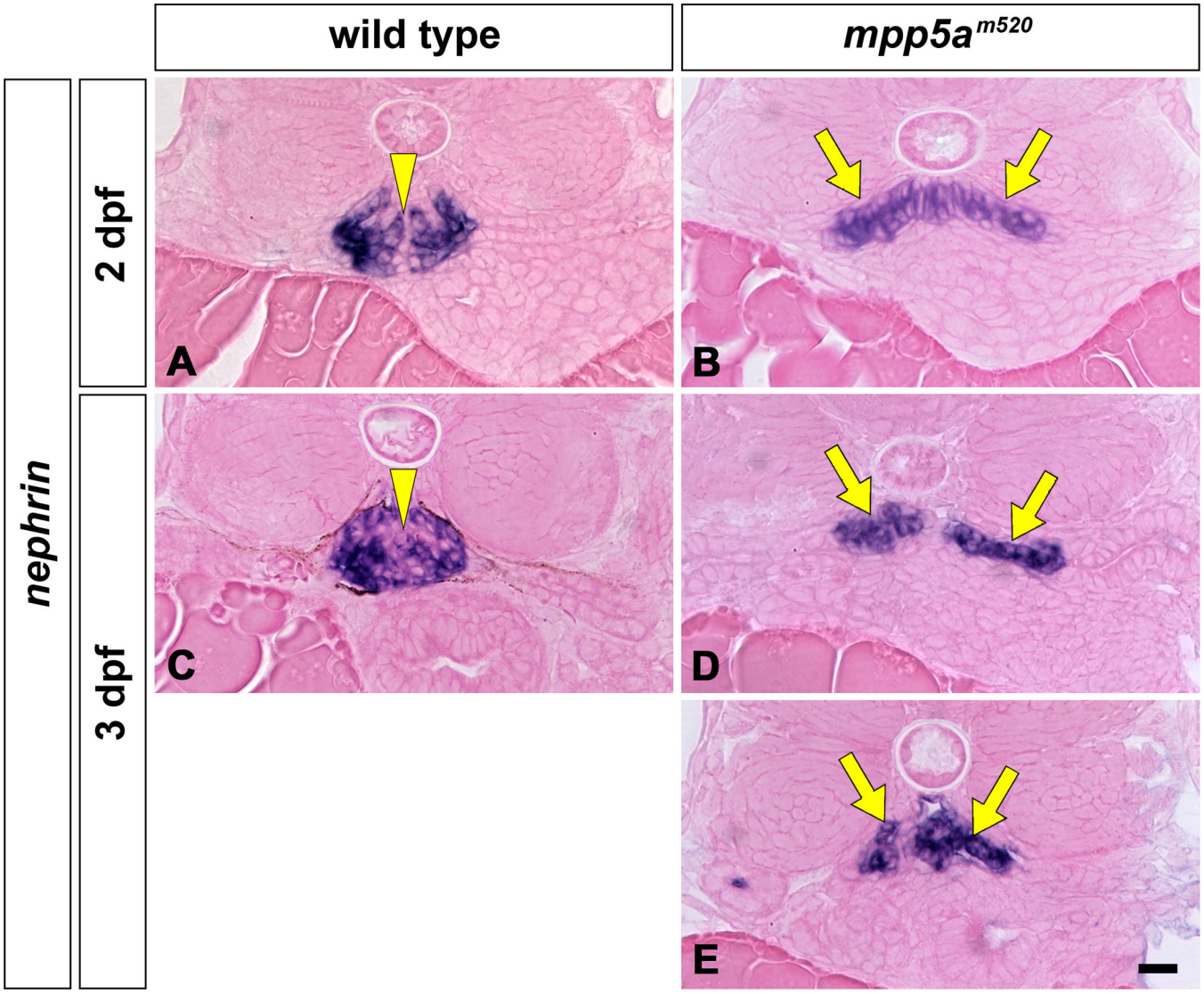

Figure 5.

nephrin mRNA expression in pronephric glomeruli of *mpp5a*^{m520} mutant. Position and shape of pronephric glomerulus are shown by *in situ* hybridization for *nephrin* mRNA at 2 dpf (A, B) and 3 dpf (C–E) which only express in podocytes. *nephrin* mRNA is expressed in the glomerulus at 2 and 3 dpf in wild-type embryos as a single globular mass beneath the notochord (A, C; arrowheads). In the *mpp5a*^{m520} mutant, the glomerulus (glomerular primordia) express *nephrin* mRNA in a domain shaped like a moustache at 2 and 3 dpf (arrows in B, D, E). Scale bar = 10 μm.

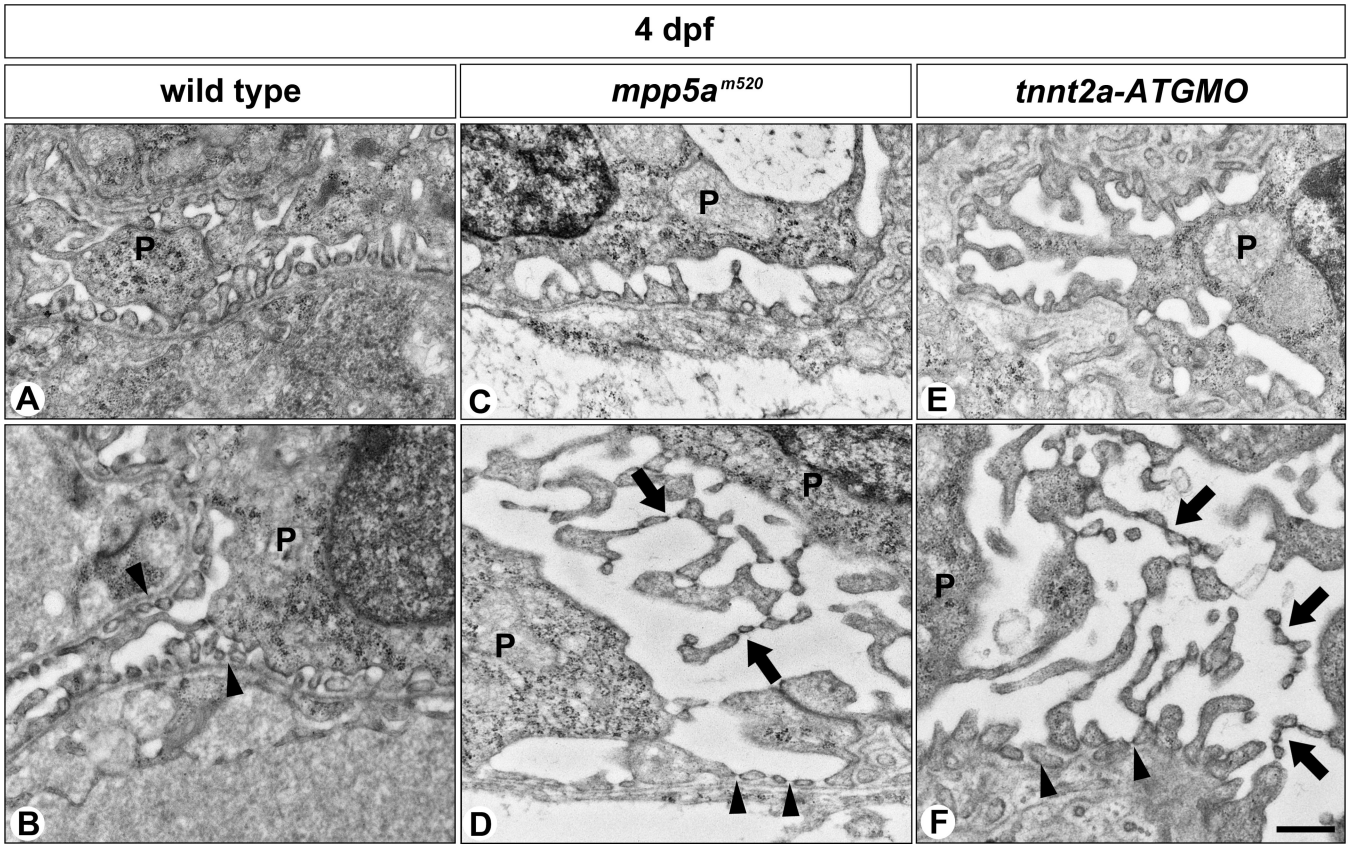

Figure 6.

Podocyte foot processes are formed in *mpp5a*^{m520} mutants and *tnnt2a-ATG* morphants. (A, B) In wild-type siblings, foot processes with SD are vigorously formed by 4 dpf. In 4 dpf *mpp5a*^{m520} mutants (C, D) and *tnnt2a-ATG* morphants (E, F) podocytes form regular foot processes with SD by 4 dpf as observed in the wild-type siblings. In most podocytes, multiple microvillus-like processes have protruded from the apical surface of the cell body and extend into the Bowman's space (arrows in D, F). In addition, they form regular foot processes adhering to the GBM (arrowheads in B, D, F). These microvillus-like processes are connected to each other by SD-like structures. P, podocyte. Scale bar = 500 nm.

$watermark-text
$watermark-text
$watermark-text

$watermark-text
$watermark-text
$watermark-text

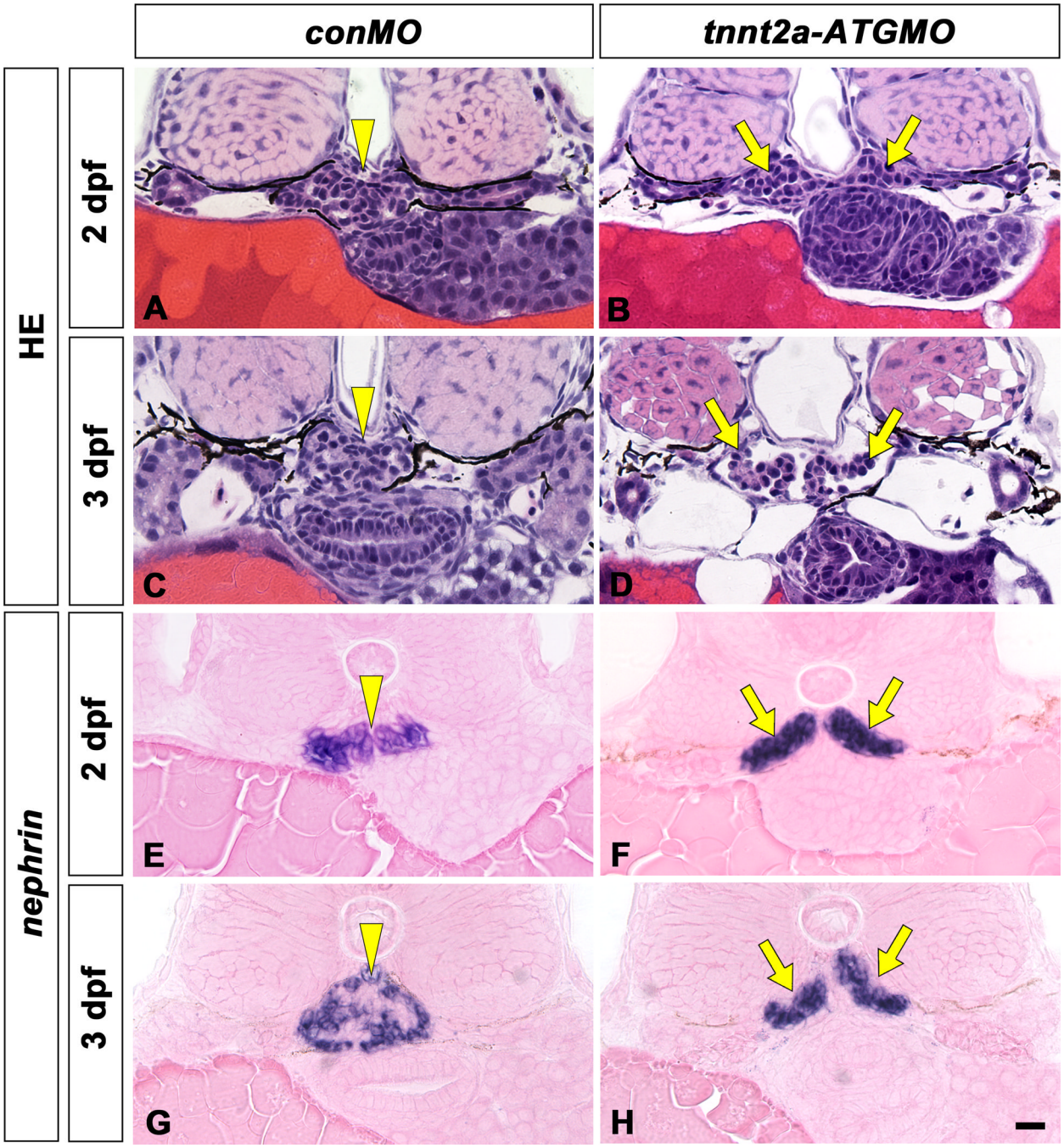

Figure 7.

A *tnnt2a-ATG* morphant displays glomerulus disorganization similar to that found in the *mpp5a*^{m520} mutants. Pronephric glomerular structure and *nephrin* mRNA expression are shown by hematoxylin-eosin stained section (A–F) and *in situ* hybridization with eosin-stained (G–J), respectively. In wild-type (A, C, E, G, I), a pair of glomerular primordia has already merged to form a single glomerulus (arrowheads) beneath the notochord at 2 dpf (A, G), 3 dpf (C, I) and 4 dpf (E). In *tnnt2a-ATG* morphants (B, D, F, H, J), a pair of glomerular primordia has retained their epithelial vesicular structure and remains unmerged at the midline in 2 dpf (arrows in B, H). Glomerular primordia have still not merged, and an extremely dilated dorsal aorta is interposed between glomerular primordia at 3 dpf (D) and 4

dpf (F). Bowman's space is apparent in the most cases of *tnnt2a-ATG* morphants (D, F). *nephrin* expressing regions are moustache-like in shape and expanded in the direction of the pronephric tubule (arrows in H, I), as is the case in the *mpp5a* mutants. Scale bar = 10 μm.

$watermark-text

$watermark-text

$watermark-text